# Genomic variation across a clinical *Cryptococcus* population linked to disease outcome

Running title: Variants and virulence in *C. neoformans*

Poppy Sephton-Clark[1], Jennifer L. Tenor[2], Dena L. Toffaletti[2], Nancy Meyers[2], Charles Giamberardino[2], Síle F. Molloy[3,4], Adrienne Chan[5], Tarsizio Chikaonda[8], Robert Heyderman[6], Mina Hosseinipour[7], Newton Kalata[8], Cecilia Kanyama[7], Christopher Kukacha[8], Duncan Lupiya[9], Henry C. Mwandumba[8], Thomas Harrison[3,4], Tihana Bicanic[3,4], John R. Perfect[2], and Christina A. Cuomo*[1]

[1]Infectious Disease and Microbiome Program, Broad Institute of MIT and Harvard, Cambridge MA 02142 USA. [2]Division of Infectious Diseases, Department of Medicine, Duke University School of Medicine, Durham, NC 27710, USA. [3]Centre for Global Health, Institute of Infection and Immunity, St George's University of London, London, United Kingdom. [4]Clinical Academic Group in Infection, St George's University Hospital, London, United Kingdom. [5]Sunnybrook Health Sciences Centre, Toronto, Canada. [6]Division of Infection and Immunity, UCL, London, United Kingdom. [7]UNC Project Malawi, University of North Carolina, USA. [8]Malawi-Liverpool-Wellcome Trust Clinical Research Programme, Blantyre, Malawi. [9]Dignitas International, Zomba, Malawi.

*Address correspondence to: Christina A. Cuomo (cuomo@broadinstitute.org)

## Abstract

*Cryptococcus neoformans* is the causative agent of cryptococcosis, a disease with poor patient outcomes, accounting for approximately 180,000 deaths each year. Patient outcomes may be impacted by the underlying genetics of the infecting isolate, however, our current understanding of how genetic diversity contributes to clinical outcomes is limited. Here, we leverage clinical, in vitro growth and genomic data for 284 *C. neoformans* isolates to identify clinically relevant pathogen variants within a population of clinical isolates from patients with HIV-associated cryptococcosis in Malawi. Through

a genome-wide association study (GWAS) approach, we identify variants associated with fungal burden and growth rate. We also find both small and large-scale variation, including aneuploidy, associated with alternate growth phenotypes, which may impact the course of infection. Genes impacted by these variants are involved in transcriptional regulation, signal transduction, glycolysis, sugar transport, and glycosylation. When combined with clinical data, we show that growth within the CNS is reliant upon glycolysis in an animal model, and likely impacts patient mortality, as CNS burden modulates patient outcome. Additionally, we find genes with roles in sugar transport are under selection in the majority of these clinical isolates. Further, we demonstrate that two hypothetical proteins identified by GWAS impact virulence in animal models. Our approach illustrates links between genetic variation and clinically relevant phenotypes, shedding light on survival mechanisms within the CNS and pathways involved in this persistence.

## Importance

Infection outcomes for cryptococcosis, most commonly caused by *C. neoformans*, are influenced by host immune responses, as well as host and pathogen genetics. Infecting yeast isolates are genetically diverse, however, we lack a deep understanding of how this diversity impacts patient outcomes. To better understand both clinical isolate diversity and how diversity contributes to infection outcome, we utilize a large collection of clinical *C. neoformans* samples, isolated from patients enrolled in a clinical trial across 3 hospitals in Malawi. By combining whole-genome sequence data, clinical data, and in vitro growth data, we utilize genome-wide association approaches to examine the genetic basis of virulence. Genes with significant associations show virulence phenotypes in both murine and rabbit models, demonstrating that our approach successfully identifies links between genetic variation and biologically significant phenotypes.

## Introduction

*Cryptococcus neoformans* is a pathogenic yeast that most commonly affects immunocompromised individuals, causing an estimated 180,000 deaths annually, with

75% of these occurring in sub-Saharan Africa. One of the leading causes of death in adults living with HIV/AIDS, cryptococcal infections are especially problematic in low-income countries where, despite a widespread roll-out of antiretroviral therapy, deaths due to opportunistic infections such as cryptococcal meningitis remain high (1). The infecting propagules of this pathogen generally enter human hosts via inhalation. From infections within the lung, *C. neoformans* may disseminate throughout the bloodstream and central nervous system of susceptible patients, causing meningitis (2). In a sample of healthcare systems across low-income countries, the 1-year mortality rate for individuals who develop cryptococcal meningitis is estimated to be 70% for those in care (uncertainty interval 59–81%) (1). A better understanding of *C. neoformans* strain virulence and fitness within the host is necessary to improve patient outcomes and develop new treatment options.

Whilst the majority of cryptococcosis cases are caused by *Cryptococcus neoformans var grubii* (3), there are often high levels of genetic diversity within clinical populations of *C. neoformans* (4–7). Furthermore, isolates of the same multilocus sequence type (MLST) have been shown to cause infections that range in severity from mild to extreme (8). To examine how genetic variation contributes to virulence phenotypes, a recent study carried out logistic regression analysis with 38 clinical *C. neoformans* isolates of the same sequence type to identify single nucleotide polymorphisms (SNPs) associated with patient survival, clinical parameters including cytokine response, immune cell counts and infection clearance, as well as in vitro data on absolute yeast growth and macrophage interactions (9). This study identified 40 candidate genes based on these association parameters, 6 of which (out of 17 genes tested) were important for survival in a murine model of *C. neoformans* infection. In a larger cohort of 230 *C. neoformans* samples from patients in South Africa, isolate sequence type was associated with patient outcome, in vitro cerebrospinal fluid (CSF) survival, and phagocytosis response (10). Full scale genome-wide association studies (GWAS) have also examined how natural variation within a *C. neoformans* population differentiates clinical and environmental isolates, identifying loss-of-function variants present in clinical *C.*

*neoformans* (VNB) populations that impact a transcription factor important for melanization, a well-studied virulence factor (11).

Furthermore, copy number variation, such as aneuploidy, has also been frequently identified within clinical populations of *C. neoformans*. Disomy of chromosome 1 is commonly reported for isolates exposed to azoles, and the higher copy number of two key genes, the *AFR1* transporter and the *ERG11* drug target, confer increased resistance to antifungals such as fluconazole (12–14). Chromosome duplication as a result of in vivo passage has also been noted in clinical isolates (15–17), and the emergence of aneuploidy in this setting has been proposed as a mechanism by which both *Cryptococcus* and *Candida* species might rapidly adapt to high-stress environments (18, 19). In *C. neoformans* aneuploidy is often transient and passage under non-selective conditions allows for reversion to euploidy (14, 17). In total, aneuploidy of chromosomes 1, 2, 4, 6, 8, 9, 10, 12, 13, and 14 have been reported in *C. neoformans* (14, 16, 17, 20–23). Despite appearing consistently throughout clinical populations, the impact of these other chromosomal aneuploidies is not yet well understood.

To better understand how genetic variation among *C. neoformans* isolates contributes to infection outcomes in patients, we carried out genome-wide association studies (GWAS) with 266 *C. neoformans* clinical isolates from the VNI lineage, selected to reduce the confounding effects of population structure between lineages. In addition to comparing selected clinical data, all isolates were also measured for in vitro growth under diverse conditions. Through our GWAS approach, we identify two hypothetical proteins associated with fungal burden in patients which also contribute to virulence in a murine model. Additionally, we show that growth in a rabbit model of CNS infection is dependent on glycolytic genes identified by GWAS, and corroborate findings that patient outcome is highly correlated with fungal burden in the CNS. Partial and full chromosomal duplications are commonly detected within this clinical population, yet these aneuploidies reduce *C. neoformans* fitness under in vitro growth conditions.

## Materials and Methods

### Sample Preparation and Sequencing

Clinical cryptococcal isolates derived from patient CSF subculture were procured through the Antifungal Combinations for Treatment of Cryptococcal Meningitis in Africa Trial (ACTA) (24); repeat cultures and duplicates were excluded. Collected strains were grown overnight in 10 ml of YPD at 30°C and 225 rpm. Genomic DNA was then extracted for sequencing with the MasterPure Yeast DNA Purification Kit, as described by Desjardins et al. (11). DNA was sheared to 250bp using a Covaris LE instrument, and adapted for Illumina sequencing as described by Fisher et al. (25). Libraries were sequenced on a HiSeq X10, generating 150bp paired reads (minimum average coverage 100x).

### Data Processing and Variant Calling

To determine sample species, reads were first aligned to a composite pan-*Cryptococcus* genome, consisting of reference genomes for *Cryptococcus neoformans var. grubii* H99, *Cryptococcus neoformans var. neoformans* JEC21, and representative genomes for lineages VGI, VGII, VGIIIa, VGIIIb, VGIV, and VGV of *Cryptococcus gattii* (26–29). To identify variants for *C. neoformans* species, reads were aligned to the *Cryptococcus neoformans var grubii* H99 reference genome (GCA_000149245.3) (27) with BWA-MEM version 0.7.17 (30). GATK v4 variant calling was carried out as documented in our publicly available cloud-based pipeline (31) (https://github.com/broadinstitute/fungal-wdl/tree/master/gatk4). Post calling, variants were filtered on the following parameters: QD < 2.0, QUAL < 30.0, SOR > 3.0, FS > 60.0 (indels > 200), MQ < 40.0, GQ < 50, alternate allele percentage = 0.8, DP < 10. Variants were annotated with SNPeff, version 4.3t (32).

### Population Genomic Analysis

A maximum likelihood phylogeny was estimated using 72,258 segregating SNP sites present in one or more isolates, allowing ambiguity in a maximum of 10% of samples, with RAxML version 8.2.12 GTRCAT rapid bootstrapping (33), and visualized with ggtree (R 3.6.0) rooted to VNII isolates. To estimate linkage disequilibrium (LD) decay,

vcftools version 0.1.16 was used to calculate LD for 1000bp windows, with a minimum minor allele frequency of 0.1, and the --hap-r2 option. Region deletions and duplications were identified using CNVnator v0.3 (significant instance e value < 0.01) (34). To identify regions under selection, composite likelihood ratio analysis was performed with PopGenome (R 3.5.0, PopGenome 2.7.5) per chromosome, by 5kb windows (35). The top 5% scoring regions (centromeric regions excluded) were tested for enrichment using a hypergeometric test with FDR correction. Large duplications and aneuploidies were visualized using funpipe (coverage analysis) version 0.1.0 (https://github.com/broadinstitute/funpipe).

**Genome-Wide Association Studies**

Association analysis between clinical data, in vitro phenotypes, and variants was carried out using PLINK v1.08p formatted files and Gemma version 0.94.1 (36) (options: centered relatedness matrix gk 1, linear mixed model), as previously described (11). Variants were considered in two scenarios, one in which rare variants (present in < 5% of the population) were collapsed by gene, and another in which loss-of-function variants (SNPeff impact high) were considered independently. Significant variants were considered to have a test score < 1.00E-6.

**Clinical Data Analysis**

De-identified clinical metadata detailing CSF fungal burden (CFU/ml), fungal clearance (EFA), patient mortality, and Glasgow coma score were provided by investigators, with these parameters determined as previously described (24). Correlation between clinical parameters was determined in R 3.6.0 with Pearson correlation coefficient, Spearman's rank correlation coefficient, point-biserial correlation, or Phi coefficient. Survival curves were generated using Prism v9.1.0 and statistics were carried out in R 3.6.0.

**In vitro Phenotyping**

Strains were grown at 30°C for two to five days. For each strain, a single colony was selected and added to 96 well microtiter plates containing 200 µL of YPD broth. Each 96 well plate contained six control strains (H99, *LAC1*, *MPK1*, *CNA1*, *RAS1*, and *HOG1*)

and a YPD control. The 96 well plates were incubated for one to two days at 30°C. Colonies were pin replicated into 384 well microtiter plates containing 80 µL of YPD broth in each well. The 384 well plates were incubated for one to two days at 30°C. They were then pinned onto one well solid agar plates in duplicate using the BM5-BC Colony Processing Robot (S & P Robotics) in 1536 array format. In three separate biological replicates, isolates were grown at 30°C, 37°C, and 39°C on YPD agar. Isolates were also pinned onto YPD+10 µg/ml fluconazole and YPD+64 µg/ml fluconazole. Images were captured after approximately 24, 48, and 72 h. Colony size at 48h was determined using gitter (37), and used to assess growth.

**Gene Deletion Strains**

Strains used for the animal studies and the primer sequences used are listed in Supplemental Table 1. KN99alpha (CM026) was used as the reference wild-type strain for deletions obtained from a genome-wide *Cryptococcus* deletion library (38). Four deletion strains were generated in wild-type *C. neoformans* strain H99 (*cnag_00544*Δ, *cnag_04102*Δ, *cnag_05324*Δ, *cnag_06033*Δ) in this study. Three DNA fragments were amplified by PCR: approximately 0.7-1 kb of 5' flank sequence, the nourseothricin (NAT) drug selection cassette amplified from pAI3 (39), and 0.7-1 kb of 3' flank sequence were prepared for each gene. The PCR products were gel extracted using the NucleoSpin Gel and PCR Clean-up Kit (Macherey-Nagel). Next, the PCR products were cloned into pUC19 using NEBuilder HiFi DNA Assembly, transformed into *Escherichia coli*, and positive plasmids were confirmed by PCR. For biolistic transformation, 2 µg of plasmid was transformed into *C. neoformans* strain H99 as previously described (40) with a slight modification that the cells were recovered on YPD containing 0.5 M sorbitol and 0.5 M mannitol. The cells were allowed to recover for 2.5 h before transferring to the selective medium, YPD+100 µg/ml NAT. Positive transformants were confirmed by PCR.

**Capsule production**

To evaluate the capsule size, capsule inducing medium (10% Sabouraud broth in 50 mM MOPS pH 7.3) was used as previously described (41). Five milliliters of capsule

inducing medium was inoculated with a single freshly streaked yeast colony and grown in an incubator shaker (225 rpm) for approximately 24 and 48 h. India ink was used as a counterstain at a 1:5 ratio (ink:cell suspension). Images were captured by microscopy (Zeis Axio Imager 1). Cell body and capsule size were measured in ImageJ V1.53a.

**Murine model of infection**

*C. neoformans* strains were grown in YPD broth at 30°C in a shaking incubator (220 rpm) for 24 h, centrifuged, and washed twice in phosphate-buffered saline (PBS). Cell counts were determined using a T4 cell counter (Nexcelom). Five male CD-1 mice (Charles River Laboratories) were infected with approximately $5 \times 10^4$ yeast cells per mouse via oropharyngeal aspiration while under isoflurane anesthesia. Mice were monitored and weighed daily. Mice with a total body weight loss of ≥ 20% or that exhibited behavioral, neurological, or respiratory symptoms were sacrificed following IACUC guidelines. Kaplan-Meier survival plots and analysis (the log-rank test) were completed using Prism software v9.1.0.; GraphPad Software. A p-value of ≤ 0.05 was considered statistically significant.

**Rabbit model of infection**

To assess the fitness and virulence of deletion strains in rabbit CSF, 3 New Zealand White male rabbits were inoculated intracisternally with 300 µl of approximately $1x10^8$ cells. Animals were sedated with ketamine and xylazine for inoculation and serial CSF cisternal taps. The rabbits were treated with hydrocortisone acetate (2.5 mg/kg) by intramuscular injections daily starting one day prior to yeast inoculation. Cisternal taps were performed on days 3, 7, and 10 followed by serial dilution of the CSF and enumeration of colonies. The time series fungal burden data were then assessed by using repeated measures analysis in R v3.6.1.

**Animal studies**

Animal experiments were performed in compliance with the Animal Welfare Act, the *Guide for the Care and Use of Laboratory Animal*s (42), and the Duke Institutional Animal Care and Use Committee (IACUC).

## Results

### The VNI lineage dominates clinical isolates and shows selection for sugar transporters

To examine variation within clinical populations, *C. neoformans* samples were isolated from HIV-infected patients as part of the ACTA trial (24), which evaluated the efficacy of fluconazole partnered with flucytosine, compared to amphotericin B combined with either fluconazole or flucytosine, as induction therapy for cryptococcal meningitis. Baseline (pre-antifungal exposure) isolates were collected from three hospitals in Malawi between 2013 and 2016. We performed whole-genome sequencing on 344 isolates and called variants against the *C. neoformans var grubii* H99 reference genome (27). Isolates identified as *Cryptococcus gattii* (45), hybrid AD *C. neoformans* (4), diploid (2), or with low coverage (9), based on evaluating read alignments to a pan-*Cryptococcus* collection of reference genomes, were removed from the analysis. To examine the population structure, a maximum likelihood phylogeny was built using 72,258 segregating SNP sites (Figure 1). Isolates can be clearly identified as VNI (266), VNII (9), and VNB (9) based on phylogenetic comparison with previously typed isolates reported by Desjardins et al (11). VNI isolates split into VNIa (217) and VNIb (49) with 100% bootstrap support; these recently described sub-lineages show strong evidence of separation (11). Of the two mating type loci found in *Cryptococcus*, mating type α predominated among these isolates, with only one VNB isolate (ACTA3525-D) possessing the alternate *MAT***a**. To assess recombination within the large VNI population, we calculated linkage disequilibrium (LD) decay and found levels of decay for lineage VNI (LD50 30kb) (Supplemental Figure 1) similar to those reported by Desjardins et al. (LD50 for VNI, VNBI, and VNBII being < 50kb) (11). There is increased decay in the VNI population as a whole when compared to individual VNIa and VNIb sub-groups (LD50 of 110kb for VNIb, LD50 not reached within 250kb for VNIa), suggesting that VNIa and VNIb isolates do not recombine exclusively within their groups.

To identify genomic regions under positive selection, we performed composite likelihood ratio analysis (43). We found that regions with scores in the top 10% in more than one

lineage (examining VNIa, VNIb, VNII, and VNB) include subtelomeric regions, centromeres, *ERG11*, and *AFR1* (Supplemental Figure 2). To examine if genes within these regions are associated with shared functions that appear under selection, we performed gene ontology (GO) enrichment analysis (Hypergeometric test, FDR correction) on regions with selection scores in the top 5% (excluding centromeres). For VNII isolates we found nucleotide excision repair enriched in these regions (corrected p-value = 6.77E-3). Sugar transport, including inositol transport, appeared robustly enriched in both VNIa and VNB lineages (corrected p-value's = 1.07E-3 and 8.60E-3), supporting previous work that identified these functions as under selection (Supplemental Table 2) (11). Sugar transport and utilization have been identified as key to success in nutrient scarce environments such as the CNS (23, 44, 45), during interactions with amoebae, and are required for virulence and resistance to external stress (46–49).

We also identified regions that were duplicated or deleted in these *C. neoformans* isolates via copy number variation analysis (Supplemental Table 3). An 8kb region was found to be duplicated in 43 VNIa isolates, containing 4 genes including a sugar transporter (TCDB: 2.A.1.1, glycerol transport), a predicted non-coding RNA, a fungal specific transcription factor (Zn2Cys6, *SIP402*), and a short-chain dehydrogenase. A separate 34kb region was found duplicated across 48 VNIa isolates encoding 11 genes including 3 dehydrogenase enzymes and 2 hydrolase enzymes. Duplicated regions unique to VNIb included an un-annotated 19kb region specific to 20 isolates and an 8kb region that encodes 2 hypothetical proteins duplicated across 21 VNIb isolates. Duplications of genes involved in resistance to azoles such as *ERG11* were found exclusively in VNII isolates, however, this did not correlate with an enhanced ability to grow in the presence of fluconazole at 64ug/ml. While these duplicated regions are not directly associated with tested phenotypes, the duplication of regions containing genes such as *ERG11* and sugar transporters may still contribute to phenotypic variation that is relevant to clinical outcomes through modulation of growth and virulence phenotypes when grown in alternate conditions.

## GWAS identifies multiple variants associated with fungal burden

We next used clinical data associated with these isolates to investigate the relationship between clinical factors, across lineages. We confirmed previous findings that mortality correlates strongly with high baseline fungal burden (CSF CFU/ml taken at diagnosis of cryptococcal meningitis) (Figure 2a, p=7.70E-7) as shown in prior studies (50–52), and observed similar outcome ratios across lineages (log-rank test, p=0.916) (Figure 2b-c), suggesting no major lineage-specific differences in virulence, though low numbers of VNB and VNII infecting isolates may limit our power to detect significant differences here. Additionally, we noted similar levels of baseline fungal burden and rates of clearance between VNIa and VNIb infecting isolates (Figure 2d-e). The data suggest a reduction in baseline fungal burden of 1.29E+06 CSF CFU/ml on average for VNII when compared to VNI isolates (Wilcoxon test, p=0.024), however, due to the limited number of VNII isolates included, this finding should be confirmed with additional cases.

To determine whether the variation in baseline fungal burden, which appears well distributed throughout this population (Figure 1), is linked to a specific genetic component, we performed genome-wide association studies (GWAS) to identify variants associated with higher fungal load, when taken as a continuous phenotype. We selected VNI isolates for this analysis as they represent the major genetic group present, and to avoid confounding factors of population structure between lineages. This analysis revealed 53 variants that were significantly (GEMMA score test, $p < 1.00E-6$) associated with CSF fungal burden levels (Figure 3a), 16 of which were predicted to result in a loss-of-function mutation. These variants impacted genes encoding 15 hypothetical proteins and 6 ncRNAs; an additional 4 variants fell into non-coding centromeric regions (Supplemental Table 4). Of the annotated genes impacted, 4 have been previously identified to modulate virulence phenotypes, these include the protein S-acyl transferase *PFA4* (CNAG_03981), the calcineurin catalytic subunit *CNA1* (CNAG_04796), and the mitochondrial co-chaperone *MRJ1* (CNAG_00938) that are required for virulence in the murine model, as well as the iron permease *FTR1* (CNAG_06242) that is required for capsule regulation (53–56). Additionally, 2 genes with variants are known to impact titan cell formation, these include the multidrug

transporter CNAG_04546 and the adenylate cyclase *CAC1* (CNAG_03202) (57, 58). A high proportion (28%) of variants with high GWAS scores (GEMMA score test, p < 1.00E-6) appeared in genes annotated as hypothetical proteins. For phenotype characterization, we decided to focus on genes impacted by variants associated with higher fungal burden, that were predicted to result in a loss-of-function within coding regions.

**Two hypothetical proteins impact virulence in a murine model**

To determine if the genes identified through our GWAS analysis of fungal burden impact virulence, we tested a total of 10 gene deletion strains across murine and rabbit models. Previous work has shown that infection outcomes from human infections are well recapitulated in murine models (8), while rabbit models have proven useful in evaluating CNS infections, as fungal burden within the CNS can be determined through longitudinal tapping of CSF (59). The most striking result from GWAS analysis was a pileup of 5 variants in the hypothetical protein CNAG_04102, with the highest scoring variant within this gene being the third most significant overall (GEMMA score test, p=1.30E-11). Deletion of CNAG_04102 in a H99 background led to reduced virulence in a murine model (5 male CD-1 mice), compared to a H99 isolate control (log-rank test, p=0.0427) (Figure 3b). This gene contains a Kyakuja-Dileera-Zisupton (KDZ) superfamily motif (pfam18758), which has been found within species from basidiomycota, mucoromycotina, *rhizophagus* and *allomyces* (60), with CNAG_04102 homologs containing this motif found in *Cryptococcus gattii* and *Cryptococcus floricola*. The KDZ motif is also commonly located within TET/JBP genes which are involved in genomic organization and epigenetic regulation (61), suggesting a role for gene expression regulation. Deletion of a second hypothetical protein, CNAG_05608, (in a CMO26 KN99 background) also resulted in reduced virulence within a murine model (5 male CD-1 mice), with isolates lacking a functional CNAG_05608 exhibiting reduced virulence, when compared to wild type (log-rank test, p=0.0154) (Figure 3c). While CNAG_05608 is annotated as a hypothetical protein, this gene is predicted to contain a single transmembrane domain and has homologs in *Cryptococcus gattii*, *Cryptococcus amylolentus*, *Kwoniella* species, and *Wallemia* species. Furthermore, this gene is

upregulated during growth in both murine and monkey lungs (62), and slightly downregulated when grown in the presence of glucose (63), suggesting a role during infection.

**Sugar transport and metabolism impacts persistence in a rabbit CNS infection model**

When loss-of-function variants were considered independently, the most highly significant variant was a frameshift in the phosphofructokinase gene, CNAG_06033 (pfkB) (GEMMA score test, p=1.69E-09). Deletion of CNAG_06033 in a H99 background resulted in significantly decreased CSF burden within the rabbit model (3 New Zealand white male rabbits) when compared to a H99 isolate, with CSF CFU/ml counts dependent on both the infecting strain and the number of days post-infection. The CSF loads were comparable across three rabbits for H99 and the CNAG_06033 deletion at 3 days post-infection, but decreased for the CNAG_06033 deletion at days 7 and 10, in contrast to the H99 isolate which showed increased CSF load over time (repeated measures analysis, p=0.0225) (Figure 3d), highlighting the need for efficient glycolysis within the mammalian CSF (44). The overall virulence within a murine model (5 male CD-1 mice) for the CNAG_06033 deletion strain appeared similar to wild type (log-rank test, p=0.1198) (Figure 3e), demonstrating that defects in glycolytic metabolism do not appear to restrict persistence and dissemination but critically may be important at specific body sites. Loss-of-function variants within this gene have been shown to emerge over the course of in vivo passage in CSF during human infection and relapse (15), suggesting a role for the loss of CNAG_06033 in adaptation to the host at specific body sites. This result is consistent with prior work that tested deletions of other genes involved in glycolysis; loss of pyruvate kinase (*pyk1Δ*) resulted in decreased persistence in the rabbit CSF, but unperturbed dissemination in a murine model (44). Further supporting the role of glycolysis and sugar transport in the survival of *C. neoformans* in CSF, we identified significant variants in additional genes involved in these pathways. A predicted xylose transporter, CNAG_05324, contained a frameshift variant present in 33 isolates (GEMMA score test, p=4.00E-07). In preliminary experiments deletion of CNAG_05324 in a H99 background led to an increase in CSF

load in one rabbit when compared to its H99 control. However, additional experiments are required to confirm these results (Supplemental Figure 3a). Given the predicted role of this gene as a xylose transporter, and the presence of xylose in cryptococcal capsule, we undertook preliminary phenotypic capsule screening of the CNAG_05324 deletion strain. Capsule analysis of this deletion mutant via cultivation in capsule-inducing media and India ink staining revealed a significant increase in capsule thickness (Welch's T-test, p=3.9E-14) (Supplemental Figure 3b), suggesting a role for CNAG_05324 in capsule size modulation. Previous work has shown that modulation of xylose transport and xylosylation can drastically alter virulence, capsule size, and immune evasion (64, 65), highlighting this capsular mechanism as an area for further exploration.

**Aneuploidy is common and slows growth**

To determine how natural variation might affect growth and other clinically relevant phenotypes, we performed in vitro phenotyping of isolates. Isolates displayed a range of growth levels on rich media (YPD) at 30°C, 37°C, and 39°C (Figure 4a-c), with colony size across conditions and replicates showing strong correlation (Figure 4d,e, replicate per condition $R^2 > 0.8$). To determine whether this variation is linked to a specific genetic component, we performed GWAS to identify variants associated with increased and decreased colony size. Significantly associated with the rapid growth of large colonies on YPD were loss-of-function variants in CNAG_06637 (UBP8 Ubiquitin-specific protease, component of the SAGA complex), CNAG_03818 (sensory transduction histidine kinase), and CNAG_10082 (tRNA Threonine) (GEMMA score test, p < 1.00E-6). A single loss-of-function variant was found significantly associated with decreased colony size, a frameshift in the dolichyldiphosphatase encoding gene, CNAG_03014 (GEMMA score test, p=9.90E-12). Naturally occurring loss-of-function variants such as these may play a role in the fitness variation we see between clinical isolates.

In addition to SNP and indel mutations, we evaluated the level of chromosome copy number variation across these clinical isolates. We observed both fully and partially duplicated chromosomes, with the most commonly duplicated chromosomes being 12,

9, 14, and 1; overall, duplication of an entire chromosome occurs in 8.5% of clinical isolates. Partial duplications, where at least 25% of the chromosome shows continuous duplication, occur most frequently in chromosomes 2 and 6 (15 instances, Figure 5a). Aneuploid isolates appear well distributed throughout this clinical dataset (Supplemental Figure 4a), suggesting frequent and independent origins for these events occurring in vivo.

To evaluate the impact of these large aneuploidies, we next compared the growth of aneuploid and euploid isolates. On rich media (YPD), at 30°C, 37°C, and 39°C, isolates harboring a fully duplicated chromosome showed significantly poorer growth than euploid isolates (Wilcoxon test, $p < 5.00E-07$), or isolates featuring only a partial chromosomal duplication (Wilcoxon test, $p < 0.01$) (Figure 5b-d). To determine whether this fitness reduction occurs in both clinical and environmental populations, we carried out a metanalysis of the data for these isolates, and data previously generated using the same assay for a diverse set of clinical and environmental isolates (Supplemental Figure 4b) (11). Isolates with aneuploidies present in both datasets displayed a significant reduction in growth on YPD at 37°C ($p=2.00E-07$), demonstrating that this reduction in fitness holds true for both clinical and environmental isolates, across lineages VNI and VNB.

Aneuploidy can be advantageous under certain stressors such as antifungal treatment, however, with optimal nutrients at a range of temperatures we found that aneuploidy significantly reduces fitness. Modulation of chromosome 1 ploidy has been linked to apoptosis-inducing factor 1 (*AIF1*) (13), however, variants within *AIF1* were not present in this population, suggesting an alternate mechanism may be responsible for modulation of chromosome copy number here.

## Discussion

Phylogenetic analysis of 284 *C. neoformans* samples from patients with cryptococcosis revealed a mixed population of VNI, VNB, and VNII isolates, dominated by the VNI lineage. We leverage clinical metadata to identify multiple variants associated with fungal burden, a factor known to impact patient mortality, in combination with additional

462 factors such as host immune response, host genetic background, and antifungal
463 treatment. We identify both SNPs and indels significantly associated with fungal burden,
464 but not with other clinical factors such as mortality and rate of yeast clearance. We
465 utilize these association results to identify three genes involved in virulence. Of these,
466 two are annotated as hypothetical proteins and when deleted show reduced virulence in
467 a murine model, and one encodes for a phosphofructokinase that when deleted shows
468 reduced persistence in a rabbit CNS model. We employ in vitro phenotyping to identify
469 multiple variants associated with both poor and prolific growth phenotypes, and through
470 copy number analysis, we reveal multiple and varied aneuploidies within this clinical
471 population, as well as a previously reported environmental population. These
472 aneuploidies appear to reduce fitness levels in isolates from both clinical and
473 environmental sources, across both VNI and VNB lineages.
474
475 Isolates collected from patients in Malawi as part of the ACTA study were dominated by
476 the VNI genetic group, the most commonly observed global lineage of *C. neoformans*.
477 This population consists of two of the three previously identified VNI lineages (VNIa,
478 and VNIb) (66, 67). VNI isolates are found around the globe and appear relatively clonal
479 when compared to the highly diverse VNB lineage, often isolated from rural niches,
480 such as mopane trees, in Africa and South America (11, 68–70).
481
482 Sugar transporters have previously been identified as under selection in both VNI and
483 VNB isolates from Botswana (11), and we find they also appear under selection in both
484 VNI and VNB isolates in this population from Malawi. Specifically, we find inositol,
485 xylose, glucose, lactose, and glucoside transporters under selection. The expansion of
486 inositol transporters in *C. neoformans* may offer an advantage in both woodland areas
487 and the CNS, as these environments have abundant inositol (46). Xylose transport is
488 important for *C. neoformans* capsule production, the variable xylosylation of which can
489 enable immune evasion (65). The signaling molecule and preferred carbon source
490 glucose, the precursor of glucoside, is known to regulate hexose transporters that are
491 required for virulence (47) and is a key glycolytic metabolite, a pathway required for
492 growth in the CNS (44).

We identified multiple variants significantly associated with clinical and growth phenotypes by taking a GWAS approach, however, clinical phenotypes such as mortality and mental-status did not show a strong association with any variants identified, perhaps due to the complex nature of these characteristics. Additionally, we used a culture-based method to select for isolates from patients, and culture-negative individuals were excluded. As a result, we were unable to detect variants associated with very low levels of fungal burden in the CNS. While extensively applied to human data, genome-wide association studies have also been applied to study fungal human pathogens (9–11) and plant-pathogens (71, 72). A major challenge is adapting these association approaches for the population structure of each species; for *C. neoformans*, while there is recombination within the population, LD50 values for VNI, VNBI, and VNBII populations are < 50kb (11). Expanding the sample size for such associations or focusing narrowly on particular genetic groups can help increase the power to detect variants, however, the choice of GWAS approach also needs to be optimized for the population under study through consideration of population structure and size.

Through analysis of the clinical metadata, we found CSF fungal burden, a measure of the quantity of live yeasts at the site of infection, to be the strongest factor in carrying out GWAS. We found that high fungal burden within the CSF of an individual strongly correlated with patient mortality, in accordance with prior work showing that high fungal load is a predictor of mortality (50–52). We found that isolates lacking a functional phosphofructokinase B (CNAG_06033) exhibited a reduced CSF load within a rabbit model; phosphofructokinase plays a key regulatory role in the glycolytic pathway. Patient isolates containing naturally occurring loss-of-function variants in CNAG_06033 showed no growth defects when grown on YPD at 37°C, and our phosphofructokinase mutant showed a CSF load reduction similar to that observed for the pyruvate kinase (*PYK1*) deletion strain within a rabbit model, likely due to the similar regulatory effects of both enzymes in glycolysis (44). Additionally, loss-of-function variants have previously been identified in CNAG_06033 (PfkB) after in vivo human passage (15). Under stress conditions, metabolically heterogeneous populations may emerge (73, 74), this

metabolic diversity might explain the emergence of isolates less reliant upon glycolysis through growth within the host. Additionally, we identified two hypothetical proteins that appear to play a role in virulence within the murine model; this highlights the power of our unbiased GWAS approach to systematically identify gene candidates implicated in virulence, in the absence of additional functional or pathway information. Other systematic studies utilizing RNA-Seq have also identified genes encoding hypothetical proteins that are strong candidates for further study, due to their high expression in CSF (23, 45). While the large proportion of *C. neoformans* genes annotated as hypothetical proteins are more challenging to study, it is critical that we more widely characterize the roles of all genes involved in the pathogenesis of *C. neoformans*.

We also found evidence that ploidy directly impacts the fitness of both clinical and environmental *C. neoformans* isolates. Aneuploidy has been linked to broad-spectrum stress resistance in *Candida* species (75), and in *C. neoformans*, disomy of chromosome 1 is known to arise in isolates treated with azoles both in vitro and in vivo and confers resistance to azoles such as fluconazole, through the increase in copy number of *AFR1* and *ERG11* (12, 14). Suggested mechanisms for modulation of chromosome 1 ploidy include regulation via the apoptosis-inducing factor Aif1 (13), however, we did not find evidence for Aif1 disruption in these isolates. Specific impacts of disomy have also been noted for chromosome 13, disomy of which results in reduced melanization (20). In *S. cerevisiae*, disomy of select chromosomes also results in reduced proliferation rates (76). Whilst the reduction in fitness we observed does not seem specific to any particular chromosome, the questions of how and why ploidy appears subject to change in stressful conditions and whether the most frequently observed aneuploidies confer a specific advantage are intriguing and will require further study.

By combining genetic, in vitro, and clinical data, we glean insights into the impact of naturally-occurring genetic variation and the implications for infection outcomes. As whole genome sequencing on an ever-larger scale becomes more accessible, and association techniques for microbial communities grow in sophistication, so too will our

555 power to detect functionally relevant genetic variation across cryptococcal populations.
556 Combined with data from large pan-African clinical trials, and approaches that leverage
557 both fungal and human variant identification, we can further dissect the interaction
558 between pathogen and host genetics. Together, this will enable a better understanding
559 of how these variations impact the ability of *Cryptococcus* to adapt to, and thrive in, the
560 wide range of environments it finds itself within.

561 **References**

562 1. Rajasingham R, Smith RM, Park BJ, Jarvis JN, Govender NP, Chiller TM, Denning
563 DW, Loyse A, Boulware DR. 2017. Global burden of disease of HIV-associated
564 cryptococcal meningitis: an updated analysis. Lancet Infect Dis 17:873–881.

565 2. Maziarz EK, Perfect JR. 2016. Cryptococcosis. Infect Dis Clin North Am 30:179–
566 206.

567 3. Chayakulkeeree M, Perfect JR. 2006. Cryptococcosis. Infect Dis Clin North Am
568 20:507–544, v–vi.

569 4. Litvintseva AP, Thakur R, Vilgalys R, Mitchell TG. 2006. Multilocus sequence
570 typing reveals three genetic subpopulations of *Cryptococcus neoformans* var.
571 *grubii* (serotype A), including a unique population in Botswana. Genetics
572 172:2223–2238.

573 5. Chen Y, Litvintseva AP, Frazzitta AE, Haverkamp MR, Wang L, Fang C, Muthoga
574 C, Mitchell TG, Perfect JR. 2015. Comparative analyses of clinical and
575 environmental populations of *Cryptococcus neoformans* in Botswana. Mol Ecol
576 24:3559–3571.

577 6. Nyazika TK, Hagen F, Machiridza T, Kutepa M, Masanganise F, Hendrickx M,
578 Boekhout T, Magombei-Majinjiwa T, Siziba N, Chin'ombe N, Mateveke K, Meis JF,
579 Robertson VJ. 2016. *Cryptococcus neoformans* population diversity and clinical
580 outcomes of HIV-associated cryptococcal meningitis patients in Zimbabwe. J Med
581 Microbiol 65:1281–1288.

582 7. Fernandes KE, Brockway A, Haverkamp M, Cuomo CA, van Ogtrop F, Perfect JR,
583 Carter DA. 2018. Phenotypic variability correlates with clinical outcome in
584 *Cryptococcus* isolates obtained from Botswanan HIV/AIDS patients. mBio
585 9(5):e02016-18.

586 8. Mukaremera L, McDonald TR, Nielsen JN, Molenaar CJ, Akampurira A, Schutz C,
587 Taseera K, Muzoora C, Meintjes G, Meya DB, Boulware DR, Nielsen K. 2019. The
588 mouse inhalation model of *Cryptococcus neoformans* infection recapitulates strain
589 virulence in humans and shows that closely related strains can possess differential
590 virulence. Infection and Immunity 87(5):e00046-19.

591 9. Gerstein AC, Jackson KM, McDonald TR, Wang Y, Lueck BD, Bohjanen S, Smith
592 KD, Akampurira A, Meya DB, Xue C, Boulware DR, Nielsen K. 2019. Identification
593 of pathogen genomic differences that impact human immune response and
594 disease during *Cryptococcus neoformans* infection. mBio 10(4):e01440-19.

595 10. Beale MA, Sabiiti W, Robertson EJ, Fuentes-Cabrejo KM, O'Hanlon SJ, Jarvis JN,
596 Loyse A, Meintjes G, Harrison TS, May RC, Fisher MC, Bicanic T. 2015. Genotypic
597 diversity Is associated with clinical outcome and phenotype in Cryptococcal
598 meningitis across southern Africa. PLOS Neglected Tropical Diseases
599 9(6):e0003847.

600 11. Desjardins CA, Giamberardino C, Sykes SM, Yu C-H, Tenor JL, Chen Y, Yang T,
601 Jones AM, Sun S, Haverkamp MR, Heitman J, Litvintseva AP, Perfect JR, Cuomo
602 CA. 2017. Population genomics and the evolution of virulence in the fungal
603 pathogen *Cryptococcus neoformans*. Genome Research 27:1207–1219.

604 12. Sionov E, Lee H, Chang YC, Kwon-Chung KJ. 2010. *Cryptococcus neoformans*
605 overcomes stress of azole drugs by formation of disomy in specific multiple
606 chromosomes. PLOS Pathogens 6(4):e1000848.

607 13. Semighini CP, Averette AF, Perfect JR, Heitman J. 2011. Deletion of *Cryptococcus*
608 *neoformans* AIF ortholog promotes chromosome aneuploidy and fluconazole-

609 resistance in a metacaspase-independent manner. PLOS Pathogens
610 7(11):e1002364.

611 14. Stone NRH, Rhodes J, Fisher MC, Mfinanga S, Kivuyo S, Rugemalila J, Segal ES,
612 Needleman L, Molloy SF, Kwon-Chung J, Harrison TS, Hope W, Berman J, Bicanic
613 T. 2019. Dynamic ploidy changes drive fluconazole resistance in human
614 cryptococcal meningitis. J Clin Invest 129:999–1014.

615 15. Chen Y, Farrer RA, Giamberardino C, Sakthikumar S, Jones A, Yang T, Tenor JL,
616 Wagih O, Van Wyk M, Govender NP, Mitchell TG, Litvintseva AP, Cuomo CA,
617 Perfect JR. 2017. Microevolution of serial clinical isolates of *Cryptococcus*
618 *neoformans* var. *grubii* and *C. gattii*. mBio 8(2):e00166-17.

619 16. Rhodes J, Beale MA, Vanhove M, Jarvis JN, Kannambath S, Simpson JA, Ryan A,
620 Meintjes G, Harrison TS, Fisher MC, Bicanic T. 2017. A population genomics
621 approach to assessing the genetic basis of within-host microevolution underlying
622 recurrent cryptococcal meningitis infection. G3: Genes, Genomes, Genetics
623 7:1165–1176.

624 17. Fu MS, Liporagi-Lopes LC, Dos SR, Júnior S, Tenor JL, Perfect JR, Cuomo CA,
625 Casadevall A. 2021. Amoeba predation of *Cryptococcus neoformans* results in
626 pleiotropic changes to traits associated with virulence. mBio 12(2):e00567-21.

627 18. Gerstein AC, Fu MS, Mukaremera L, Li Z, Ormerod KL, Fraser JA, Berman J,
628 Nielsen K. 2015. Polyploid titan cells produce haploid and aneuploid progeny to
629 promote stress adaptation. mBio 6(5):e01340-15.

630 19. Berman J. 2016. Ploidy plasticity: a rapid and reversible strategy for adaptation to
631 stress. FEMS Yeast Research 16(3):fow020.

632 20. Hu G, Wang J, Choi J, Jung WH, Liu I, Litvintseva AP, Bicanic T, Aurora R, Mitchell
633 TG, Perfect JR, Kronstad JW. 2011. Variation in chromosome copy number
634 influences the virulence of *Cryptococcus neoformans* and occurs in isolates from
635 AIDS patients. BMC Genomics 12:526.

21. Ormerod KL, Morrow CA, Chow EWL, Lee IR, Arras SDM, Schirra HJ, Cox GM, Fries BC, Fraser JA. 2013. Comparative genomics of serial isolates of *Cryptococcus neoformans* reveals gene associated with carbon utilization and virulence. G3: Genes, Genomes, Genetics 3:675–686.

22. Rhodes J, Desjardins CA, Sykes SM, Beale MA, Vanhove M, Sakthikumar S, Chen Y, Gujja S, Saif S, Chowdhary A, Lawson DJ, Ponzio V, Colombo AL, Meyer W, Engelthaler DM, Hagen F, Illnait-Zaragozi MT, Alanio A, Vreulink JM, Heitman J, Perfect JR, Litvintseva AP, Bicanic T, Harrison TS, Fisher MC, Cuomo CA. 2017. Tracing genetic exchange and biogeography of *Cryptococcus neoformans* var. *grubii* at the global population level. Genetics 207:327–346.

23. Yu C-H, Sephton-Clark P, Tenor JL, Toffaletti D, Giamberardino C, Haverkamp M, Cuomo C, Perfect J. 2021. Gene expression of diverse *Cryptococcus* isolates during infection of the human central nervous system. mBio 12(6):e0231321.

24. Molloy SF, Kanyama C, Heyderman RS, Loyse A, Kouanfack C, Chanda D, Mfinanga S, Temfack E, Lakhi S, Lesikari S, Chan AK, Stone N, Kalata N, Karunaharan N, Gaskell K, Peirse M, Ellis J, Chawinga C, Lontsi S, Ndong J-G, Bright P, Lupiya D, Chen T, Bradley J, Adams J, van der Horst C, van Oosterhout JJ, Sini V, Mapoure YN, Mwaba P, Bicanic T, Lalloo DG, Wang D, Hosseinipour MC, Lortholary O, Jaffar S, Harrison TS, ACTA Trial Study Team. 2018. Antifungal combinations for treatment of cryptococcal meningitis in Africa. N Engl J Med 378:1004–1017.

25. Fisher S, Barry A, Abreu J, Minie B, Nolan J, Delorey TM, Young G, Fennell TJ, Allen A, Ambrogio L, Berlin AM, Blumenstiel B, Cibulskis K, Friedrich D, Johnson R, Juhn F, Reilly B, Shammas R, Stalker J, Sykes SM, Thompson J, Walsh J, Zimmer A, Zwirko Z, Gabriel S, Nicol R, Nusbaum C. 2011. A scalable, fully automated process for construction of sequence-ready human exome targeted capture libraries. Genome Biology 12(1):R1.

663 26. Loftus BJ, Fung E, Roncaglia P, Rowley D, Amedeo P, Bruno D, Vamathevan J,
664 Miranda M, Anderson IJ, Fraser JA, Allen JE, Bosdet IE, Brent MR, Chiu R,
665 Doering TL, Donlin MJ, D'Souza CA, Fox DS, Grinberg V, Fu J, Fukushima M,
666 Haas BJ, Huang JC, Janbon G, Jones SJM, Koo HL, Krzywinski MI, Kwon-Chung
667 JK, Lengeler KB, Maiti R, Marra MA, Marra RE, Mathewson CA, Mitchell TG,
668 Pertea M, Riggs FR, Salzberg SL, Schein JE, Shvartsbeyn A, Shin H, Shumway M,
669 Specht CA, Suh BB, Tenney A, Utterback TR, Wickes BL, Wortman JR, Wye NH,
670 Kronstad JW, Lodge JK, Heitman J, Davis RW, Fraser CM, Hyman RW. 2005. The
671 genome of the basidiomycetous yeast and human pathogen *Cryptococcus*
672 *neoformans*. Science 307:1321–1324.

673 27. Janbon G, Ormerod KL, Paulet D, Byrnes EJ, Yadav V, Chatterjee G, Mullapudi N,
674 Hon CC, Billmyre RB, Brunel F, Bahn YS, Chen W, Chen Y, Chow EWL, Coppée
675 JY, Floyd-Averette A, Gaillardin C, Gerik KJ, Goldberg J, Gonzalez-Hilarion S,
676 Gujja S, Hamlin JL, Hsueh YP, Ianiri G, Jones S, Kodira CD, Kozubowski L, Lam
677 W, Marra M, Mesner LD, Mieczkowski PA, Moyrand F, Nielsen K, Proux C,
678 Rossignol T, Schein JE, Sun S, Wollschlaeger C, Wood IA, Zeng Q, Neuvéglise C,
679 Newlon CS, Perfect JR, Lodge JK, Idnurm A, Stajich JE, Kronstad JW, Sanyal K,
680 Heitman J, Fraser JA, Cuomo CA, Dietrich FS. 2014. Analysis of the Genome and
681 Transcriptome of *Cryptococcus neoformans* var. *grubii* reveals complex RNA
682 expression and microevolution leading to virulence attenuation. PLoS Genetics
683 10(4):e1004261.

684 28. Farrer RA, Desjardins CA, Sakthikumar S, Gujja S, Saif S, Zeng Q, Chen Y, Voelz
685 K, Heitman J, May RC, Fisher MC, Cuomo CA. 2015. Genome evolution and
686 innovation across the four major lineages of *Cryptococcus gattii*. mBio
687 6(5):e00868-15.

688 29. Farrer RA, Chang M, Davis MJ, van Dorp L, Yang DH, Shea T, Sewell TR, Meyer
689 W, Balloux F, Edwards HM, Chanda D, Kwenda G, Vanhove M, Chang YC, Cuomo
690 CA, Fisher MC, Kwon-Chung KJ. 2019. A new lineage of *Cryptococcus gattii* (VGV)
691 discovered in the central zambezian miombo woodlands. mBio 10(6):e02306-19.

692 30. Li H. 2013. Aligning sequence reads, clone sequences and assembly contigs with
693 BWA-MEM. arXiv:13033997 [q-bio].

694 31. Van der Auwera GA, Carneiro MO, Hartl C, Poplin R, Del Angel G, Levy-
695 Moonshine A, Jordan T, Shakir K, Roazen D, Thibault J, Banks E, Garimella KV,
696 Altshuler D, Gabriel S, DePristo MA. 2013. From FastQ data to high confidence
697 variant calls: the Genome Analysis Toolkit best practices pipeline. Curr Protoc
698 Bioinformatics 43:11.10.1-11.10.33.

699 32. Cingolani P, Platts A, Wang LL, Coon M, Nguyen T, Wang L, Land SJ, Lu X,
700 Ruden DM. 2012. A program for annotating and predicting the effects of single
701 nucleotide polymorphisms, SnpEff: SNPs in the genome of *Drosophila*
702 *melanogaster* strain w $^{1118}$ ; iso-2; iso-3. Fly 6:80–92.

703 33. Stamatakis A. 2014. RAxML version 8: a tool for phylogenetic analysis and post-
704 analysis of large phylogenies. Bioinformatics 30:1312–1313.

705 34. Abyzov A, Urban AE, Snyder M, Gerstein M. 2011. CNVnator: An approach to
706 discover, genotype, and characterize typical and atypical CNVs from family and
707 population genome sequencing. Genome Res 21:974–984.

708 35. Pfeifer B, Wittelsbürger U, Ramos-Onsins SE, Lercher MJ. 2014. PopGenome: an
709 efficient Swiss army knife for population genomic analyses in R. Mol Biol Evol
710 31:1929–1936.

711 36. Zhou X, Stephens M. 2012. Genome-wide efficient mixed-model analysis for
712 association studies. 7. Nature Genetics 44:821–824.

713 37. Wagih O, Parts L. 2014. gitter: A robust and accurate method for quantification of
714 colony sizes from plate images. G3 (Bethesda) 4:547–552.

715 38. Chun CD, Madhani HD. 2010. Applying genetics and molecular biology to the study
716 of the human pathogen *Cryptococcus neoformans*. Methods Enzymol 470:797–
717 831.

718 39. Idnurm A, Reedy JL, Nussbaum JC, Heitman J. 2004. *Cryptococcus neoformans*
719 virulence gene discovery through insertional mutagenesis. Eukaryot Cell 3:420–
720 429.

721 40. Toffaletti DL, Rude TH, Johnston SA, Durack DT, Perfect JR. 1993. Gene transfer
722 in *Cryptococcus neoformans* by use of biolistic delivery of DNA. J Bacteriol
723 175:1405–1411.

724 41. Zaragoza O, Casadevall A. 2004. Experimental modulation of capsule size in
725 *Cryptococcus neoformans*. Biol Proced Online 6:10–15.

726 42. National Research Council (US) Committee for the Update of the Guide for the
727 Care and Use of Laboratory Animals. 2011. Guide for the Care and Use of
728 Laboratory Animals, 8th ed. National Academies Press (US), Washington (DC).

729 43. Nielsen R, Williamson S, Kim Y, Hubisz MJ, Clark AG, Bustamante C. 2005.
730 Genomic scans for selective sweeps using SNP data. Genome Res 15:1566–1575.

731 44. Price MS, Betancourt-Quiroz M, Price JL, Toffaletti DL, Vora H, Hu G, Kronstad
732 JW, Perfect JR. 2011. *Cryptococcus neoformans* requires a functional glycolytic
733 pathway for disease but not persistence in the host. mBio 2(3):e00103-e111.

734 45. Chen Y, Toffaletti DL, Tenor JL, Litvintseva AP, Fang C, Mitchell TG, McDonald
735 TR, Nielsen K, Boulware DR, Bicanic T, Perfect JR. 2014. The *Cryptococcus*
736 *neoformans* transcriptome at the site of human meningitis. mBio 5(1):e01087-13.

737 46. Xue C, Liu T, Chen L, Li W, Liu I, Kronstad JW, Seyfang A, Heitman J. 2010. Role
738 of an expanded inositol transporter repertoire in *Cryptococcus neoformans* sexual
739 reproduction and virulence. mBio 1(1):e00084-10.

740 47. Liu T-B, Wang Y, Baker GM, Fahmy H, Jiang L, Xue C. 2013. The glucose sensor-
741 like protein Hxs1 Is a high-affinity glucose transporter and required for virulence in
742 *Cryptococcus neoformans*. PLOS ONE 8(5):e64239.

48. Li LX, Rautengarten C, Heazlewood JL, Doering TL. 2018. UDP-Glucuronic acid transport is required for virulence of *Cryptococcus neoformans*. mBio 9(1):e02319-17.

49. Li LX, Rautengarten C, Heazlewood JL, Doering TL. 2018. Xylose donor transport is critical for fungal virulence. PLOS Pathogens 14(1):e1006765.

50. Brouwer AE, Rajanuwong A, Chierakul W, Griffin GE, Larsen RA, White NJ, Harrison TS. 2004. Combination antifungal therapies for HIV-associated cryptococcal meningitis: a randomised trial. Lancet 363:1764–1767.

51. Bicanic T, Muzoora C, Brouwer AE, Meintjes G, Longley N, Taseera K, Rebe K, Loyse A, Jarvis J, Bekker L-G, Wood R, Limmathurotsakul D, Chierakul W, Stepniewska K, White NJ, Jaffar S, Harrison TS. 2009. Independent association between rate of clearance of infection and clinical outcome of HIV-associated cryptococcal meningitis: analysis of a combined cohort of 262 patients. Clin Infect Dis 49:702–709.

52. Jarvis JN, Bicanic T, Loyse A, Namarika D, Jackson A, Nussbaum JC, Longley N, Muzoora C, Phulusa J, Taseera K, Kanyembe C, Wilson D, Hosseinipour MC, Brouwer AE, Limmathurotsakul D, White N, van der Horst C, Wood R, Meintjes G, Bradley J, Jaffar S, Harrison T. 2014. Determinants of mortality in a combined cohort of 501 patients with HIV-associated Cryptococcal meningitis: implications for improving outcomes. Clin Infect Dis 58:736–745.

53. Jung WH, Sham A, Lian T, Singh A, Kosman DJ, Kronstad JW. 2008. Iron source preference and regulation of iron uptake in *Cryptococcus neoformans*. PLOS Pathogens 4(2):e45.

54. Nichols CB, Ost KS, Grogan DP, Pianalto K, Hasan S, Alspaugh JA. 2015. Impact of protein palmitoylation on the virulence potential of *Cryptococcus neoformans*. Eukaryotic Cell 14:626–635.

769 55. Fu C, Donadio N, Cardenas ME, Heitman J. 2018. Dissecting the roles of the
770 calcineurin pathway in unisexual reproduction, stress responses, and virulence in
771 *Cryptococcus deneoformans*. Genetics 208:639–653.

772 56. Horianopoulos LC, Hu G, Caza M, Schmitt K, Overby P, Johnson JD, Valerius O,
773 Braus GH, Kronstad JW. 2020. The novel J-Domain protein Mrj1 is required for
774 mitochondrial respiration and virulence in *Cryptococcus neoformans*. mBio
775 11(3):e01127-20.

776 57. Okagaki LH, Wang Y, Ballou ER, O'Meara TR, Bahn Y-S, Alspaugh JA, Xue C,
777 Nielsen K. 2011. Cryptococcal titan cell formation is regulated by G-Protein
778 signaling in response to multiple stimuli. Eukaryot Cell 10:1306–1316.

779 58. Trevijano-Contador N, Oliveira HC de, García-Rodas R, Rossi SA, Llorente I,
780 Zaballos Á, Janbon G, Ariño J, Zaragoza Ó. 2018. *Cryptococcus neoformans* can
781 form titan-like cells in vitro in response to multiple signals. PLOS Pathogens
782 14(5):e1007007.

783 59. Perfect JR, Lang SD, Durack DT. 1980. Chronic cryptococcal meningitis: a new
784 experimental model in rabbits. Am J Pathol 101:177–194.

785 60. Muszewska A, Steczkiewicz K, Stepniewska-Dziubinska M, Ginalski K. 2017. Cut-
786 and-paste transposons in fungi with diverse lifestyles. Genome Biology and
787 Evolution 9:3463–3477.

788 61. Iyer LM, Zhang D, de Souza RF, Pukkila PJ, Rao A, Aravind L. 2014. Lineage-
789 specific expansions of TET/JBP genes and a new class of DNA transposons shape
790 fungal genomic and epigenetic landscapes. Proc Natl Acad Sci USA 111:1676–
791 1683.

792 62. Li H, Li Y, Sun T, Du W, Li C, Suo C, Meng Y, Liang Q, Lan T, Zhong M, Yang S,
793 Niu C, Li D, Ding C. 2019. Unveil the transcriptional landscape at the
794 *Cryptococcus*-host axis in mice and nonhuman primates. PLOS Neglected Tropical
795 Diseases 13(7):e0007566.

796 63. Burke JE, Longhurst AD, Merkurjev D, Sales-Lee J, Rao B, Moresco JJ, Yates JR,
797 Li JJ, Madhani HD. 2018. Spliceosome profiling visualizes operations of a dynamic
798 RNP at nucleotide resolution. Cell 173:1014-1030.e17.

799 64. Moyrand F, Klaproth B, Himmelreich U, Dromer F, Janbon G. 2002. Isolation and
800 characterization of capsule structure mutant strains of *Cryptococcus neoformans*.
801 Mol Microbiol 45:837–849.

802 65. Li LX, Hole CR, Rangel-Moreno J, Khader SA, Doering TL. 2020. *Cryptococcus*
803 *neoformans* evades pulmonary immunity by modulating xylose precursor transport.
804 Infect Immun 88(8):e00288-20.

805 66. Vanhove M, Beale MA, Rhodes J, Chanda D, Lakhi S, Kwenda G, Molloy S,
806 Karunaharan N, Stone N, Harrison TS, Bicanic T, Fisher MC. 2017. Genomic
807 epidemiology of *Cryptococcus* yeasts identifies adaptation to environmental niches
808 underpinning infection across an African HIV/AIDS cohort. Molecular Ecology
809 26:1991–2005.

810 67. Ashton PM, Thanh LT, Trieu PH, Van Anh D, Trinh NM, Beardsley J, Kibengo F,
811 Chierakul W, Dance DAB, Rattanavong S, Davong V, Hung LQ, Chau NVV, Tung
812 NLN, Chan AK, Thwaites GE, Lalloo DG, Anscombe C, Nhat LTH, Perfect J,
813 Dougan G, Baker S, Harris S, Day JN. 2019. Three phylogenetic groups have
814 driven the recent population expansion of *Cryptococcus neoformans*. Nature
815 Communications 10(1):2035.

816 68. Litvintseva AP, Carbone I, Rossouw J, Thakur R, Govender NP, Mitchell TG. 2011.
817 Evidence that the human pathogenic fungus *Cryptococcus neoformans* var. *grubii*
818 may have evolved in Africa. PLoS ONE 6(5):e19688.

819 69. Khayhan K, Hagen F, Pan W, Simwami S, Fisher MC, Wahyuningsih R,
820 Chakrabarti A, Chowdhary A, Ikeda R, Taj-Aldeen SJ, Khan Z, Ip M, Imran D, Sjam
821 R, Sriburee P, Liao W, Chaicumpar K, Vuddhakul V, Meyer W, Trilles L, Iersel LJJ
822 van, Meis JF, Klaassen CHW, Boekhout T. 2013. Geographically structured

populations of *Cryptococcus neoformans* variety *grubii* in Asia correlate with HIV status and show a clonal population structure. PLOS ONE 8:e72222.

70. Andrade-Silva LE, Ferreira-Paim K, Ferreira TB, Vilas-Boas A, Mora DJ, Manzato VM, Fonseca FM, Buosi K, Andrade-Silva J, Prudente B da S, Araujo NE, Sales-Campos H, Silva MV da, Júnior VR, Meyer W, Silva-Vergara ML. 2018. Genotypic analysis of clinical and environmental *Cryptococcus neoformans* isolates from Brazil reveals the presence of VNB isolates and a correlation with biological factors. PLOS ONE 13(3):e0193237.

71. Palma-Guerrero J, Hall CR, Kowbel D, Welch J, Taylor JW, Brem RB, Glass NL. 2013. Genome wide association identifies novel loci involved in fungal communication. PLoS Genetics 9(8):e1003669.

72. Gao Y, Liu Z, Faris JD, Richards J, Brueggeman RS, Li X, Oliver RP, McDonald BA, Friesen TL. 2016. Validation of genome-wide association studies as a tool to identify virulence factors in *Parastagonospora nodorum*. Phytopathology 106:1177–1185.

73. Alanio A, Vernel-Pauillac F, Sturny-Leclère A, Dromer F. 2015. *Cryptococcus neoformans* host adaptation: toward biological evidence of dormancy. mBio 6(2):e02580-14.

74. Hommel B, Sturny-Leclère A, Volant S, Veluppillai N, Duchateau M, Yu C-H, Hourdel V, Varet H, Matondo M, Perfect JR, Casadevall A, Dromer F, Alanio A. 2019. *Cryptococcus neoformans* resists to drastic conditions by switching to viable but non-culturable cell phenotype. PLOS Pathogens 15(7):e1007945.

75. Yang F, Teoh F, Tan ASM, Cao Y, Pavelka N, Berman J. 2019. Aneuploidy enables cross-adaptation to unrelated drugs. Molecular Biology and Evolution 36:1768–1782.

76. Torres EM, Sokolsky T, Tucker CM, Chan LY, Boselli M, Dunham MJ, Amon A. 2007. Effects of aneuploidy on cellular physiology and cell division in haploid yeast. Science 317:916–924.

## Data Availability

Isolate sequence data can be accessed in NCBI via accession PRJNA764746.

## Ethics

The ACTA trial from which the isolates described here were collected had ethical approval from the London School of Hygiene and Tropical Medicine Research Ethics Committee and by all the site national research ethics committees and regulatory bodies. De-identified clinical metadata (fungal burden, fungal clearance (EFA), patient outcome) was provided by investigators for analysis performed here.

## Acknowledgments

We thank the Broad Institute Genomics Platform for generating the sequence data for this study. We thank all of the patients and their families, as well as the staff at all the sites not directly involved in the ACTA trial; Andrew Nunn, Halima Dawood, Andrew Kitua, and William Powderly for serving on the data and safety monitoring committee; Graeme Meintjes, Calice Talom, Newton Kumwenda, and Maryline Bonnet for serving on the trial steering committee; and the ANRS Staff in Paris (Brigitte Bazin, Claire Rekacewicz, and Paula Garcia) for constant support.

## Funding

This project has been funded in part with Federal funds from the National Institute of Allergy and Infectious Diseases, National Institutes of Health, Department of Health and Human Services, under award U19AI110818 to the Broad Institute and Public Health Service Grants AI73896 and AI93257 to JRP. CAC is a CIFAR fellow in the Fungal Kingdom Program. RSH is a NIHR Senior Investigator. The views expressed in this

874 publication are those of the author(s) and not necessarily those of the NIHR or the
875 Department of Health and Social Care.

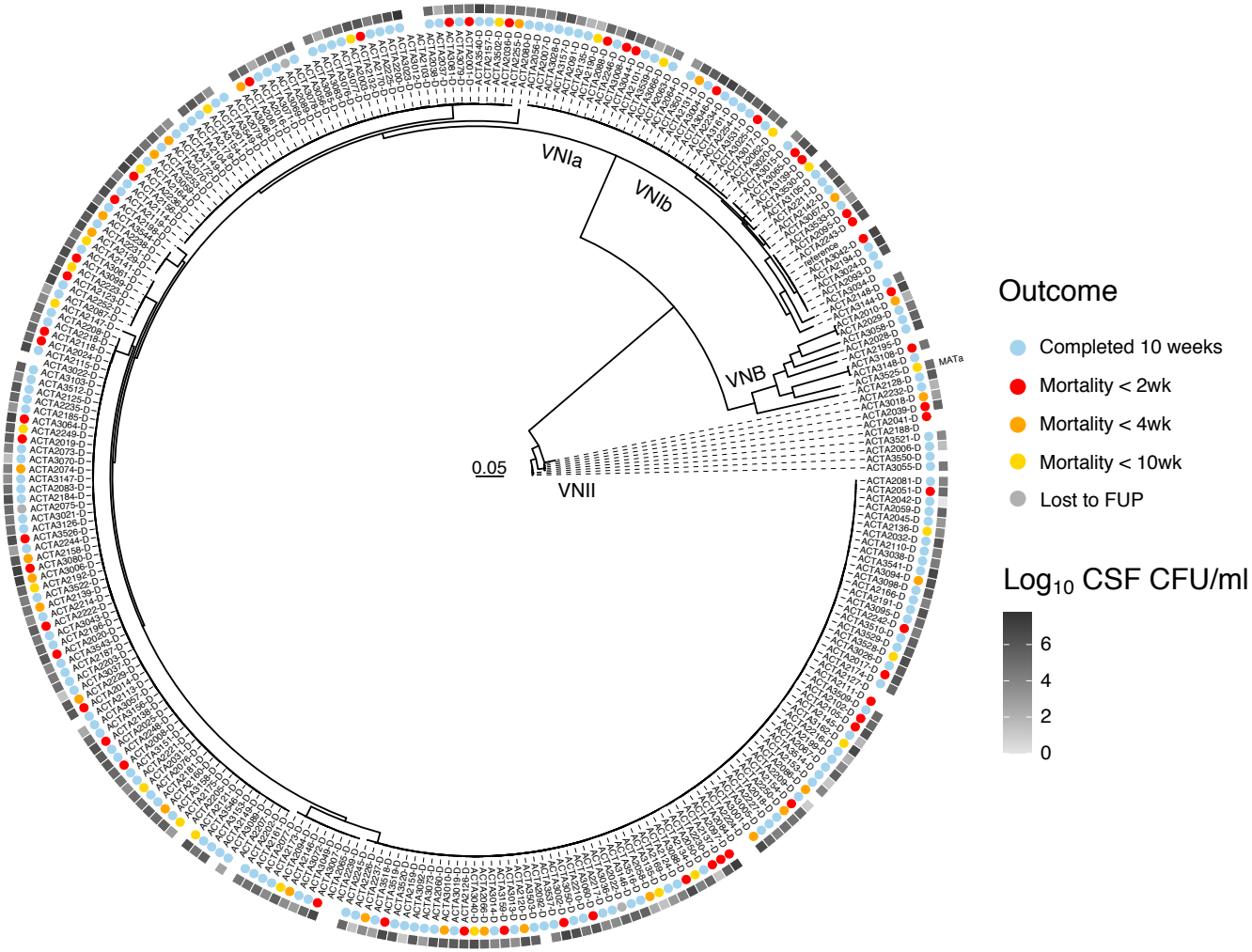


Figure 1. Maximum likelihood phylogeny of patient isolates, estimated from 72,258 segregating SNP sites, rooted to VNII. Isolates separate distinctly into VNI, VNB, and VNII, with all lineages having 100% bootstrap support. All isolates possess MAT$\alpha$ except ACTA3523 (highlighted). Colored circles correspond to patient survival. Greyscale squares indicate patient fungal burden of cerebrospinal fluid prior to treatment, Log10(CFU/ml).

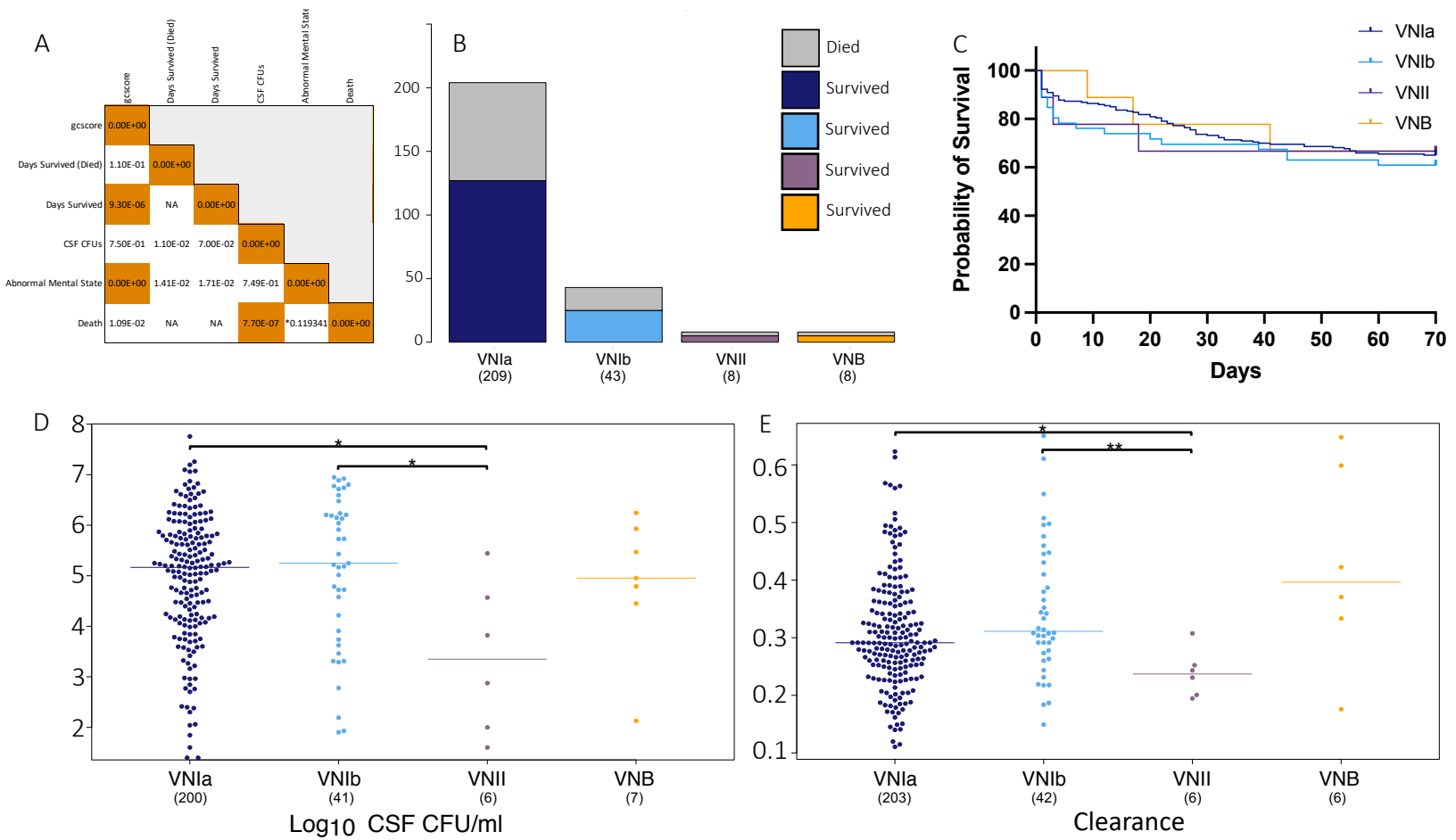


Figure 2. A) Correlation coefficient between clinical phenotypes, $p < 0.0001$ in orange. Asterisk indicates phi coefficient. Days survived indicates the total number of days survived for all individuals. Days survived (Died) indicates the number of days survived only for individuals that died during the ACTA clinical trial. B) Deaths (top, grey) and survival (bottom) of patients by infecting isolate lineage. C) Probability of survival, by lineage of infecting isolate. D) $Log_{10}$ CSF CFU/ml (fungal burden) by infecting isolate lineage, asterisk indicates $p < 0.05$, Wilcoxon test. E) Rate of clearance (EFA) by infecting isolate lineage. Displayed as -1(gradient), asterisk indicates $p < 0.05$ and 0.01, Wilcoxon test.

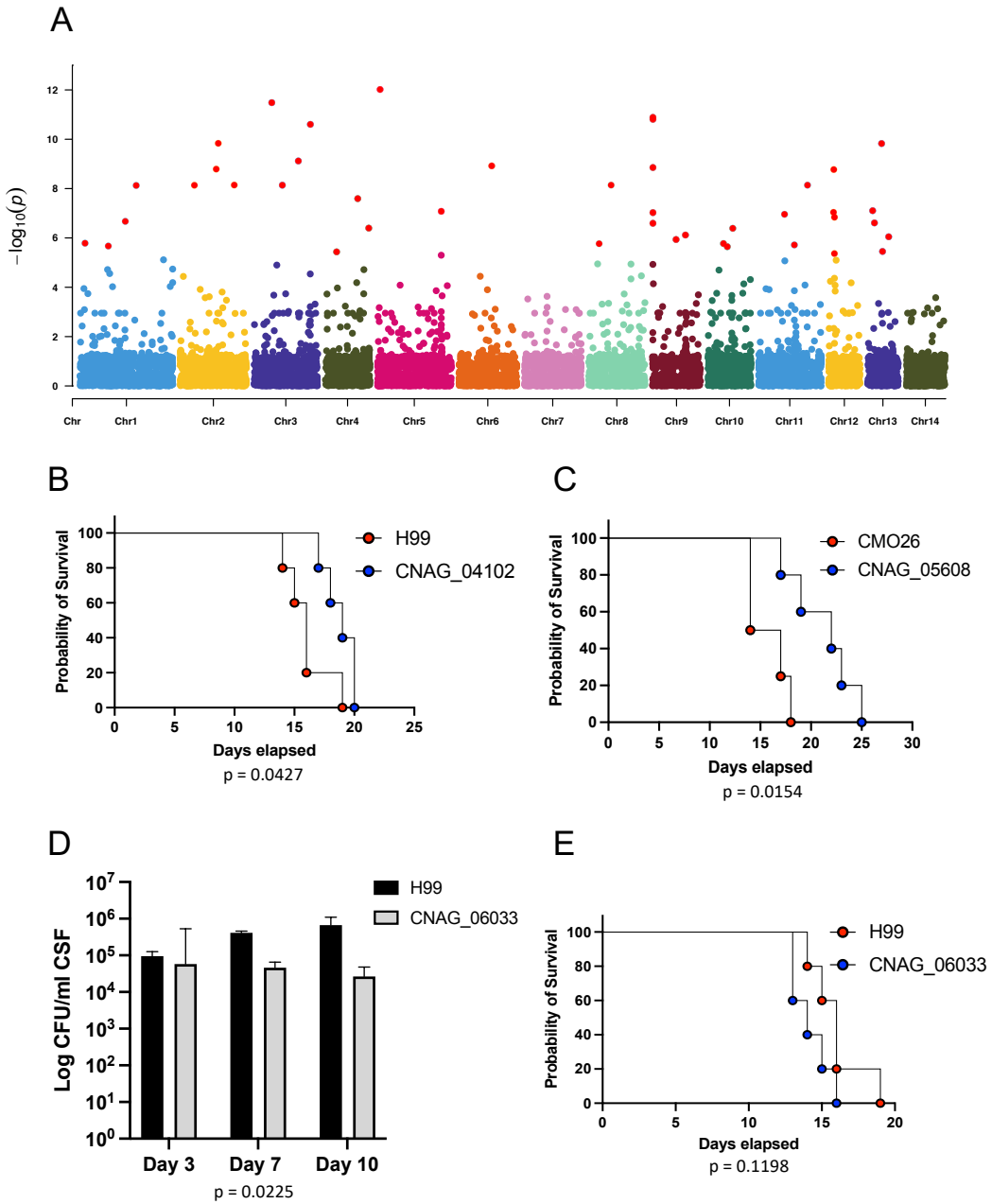


Figure 3. A) Manhattan plot displaying variants associated with high fungal burden. Variants with an association score < 0.000005 (score test) are labeled in red. B) Survival of mice infected with parental strain (H99) and a CNAG_04102 mutant strain. Five CD-1 mice were infected with approximately $5x10^4$ CFU by oropharyngeal aspiration. C) Survival of mice infected with parental strain (CM026) and a CNAG_05608 mutant strain. Five CD-1 mice were infected with approximately $5x10^4$ CFU by oropharyngeal aspiration. One mouse infected with CNAG_05608 was excluded from analysis as an outlier. At Day 45 of infection, this mouse was assessed for fungal burden in the lung and brain and both tissues were sterile. D) Rabbit CSF CFU's for the parental strain (H99) and a CNAG_06033 mutant strain extracted on days 3, 7, and 10 post-infection. Three rabbits were infected per strain. E) Survival of mice infected with parental strain (H99) and a CNAG_06033 mutant strain. Five CD-1 mice were infected with approximately $5x10^4$ CFU by oropharyngeal aspiration.

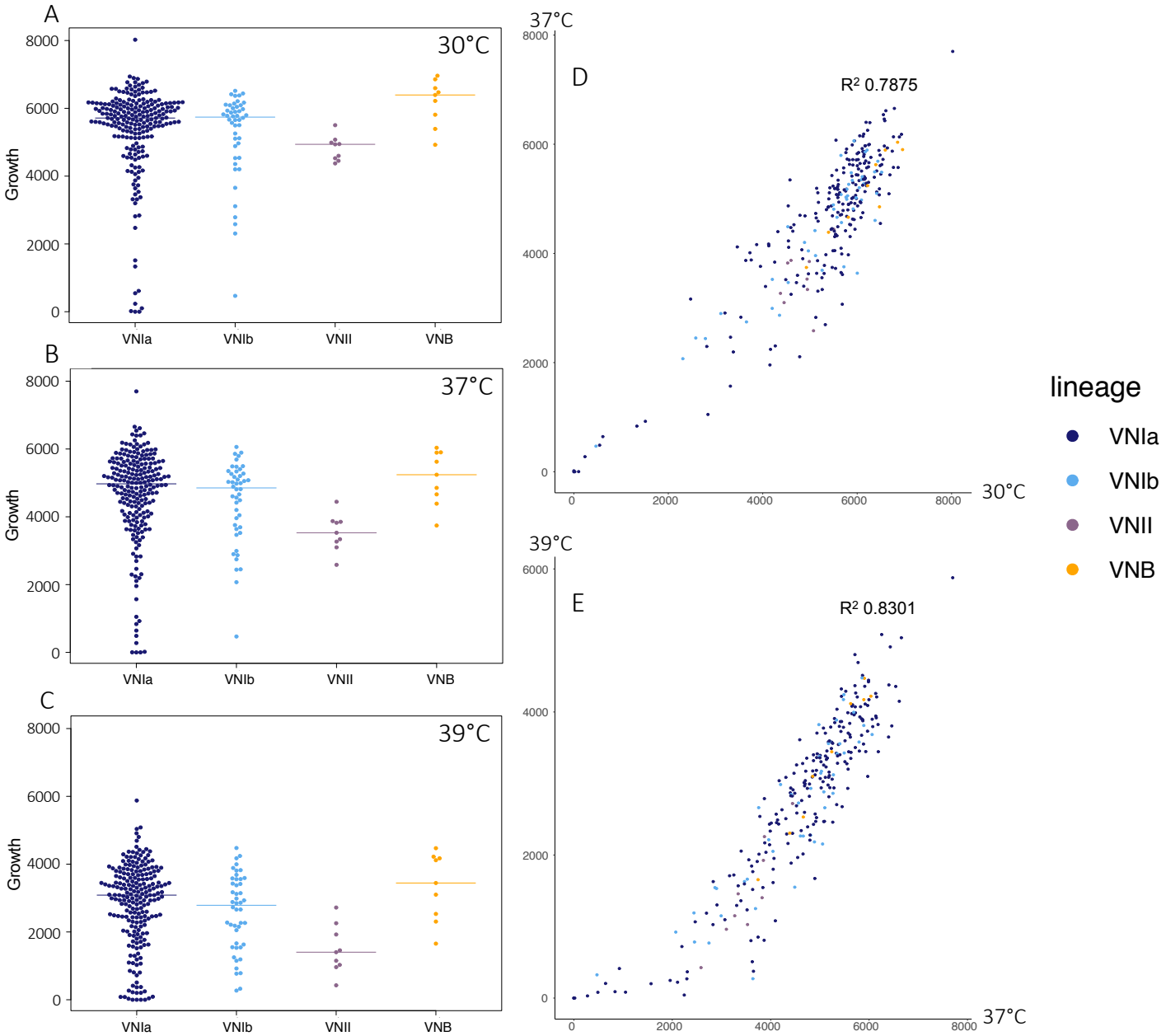


Figure 4. Colony size (area, px) of isolates grown on YPD at A) 30°C, B) 37°C, C) 39°C. Correlation of isolate growth (area, px) on YPD, with axes corresponding to colony size when grown at D) 30°C and 37°C, E) 37°C and 39°C. Colors correspond to isolate lineage: VNIa (dark blue), VNIb (light blue), VNII (purple), VNB (orange).

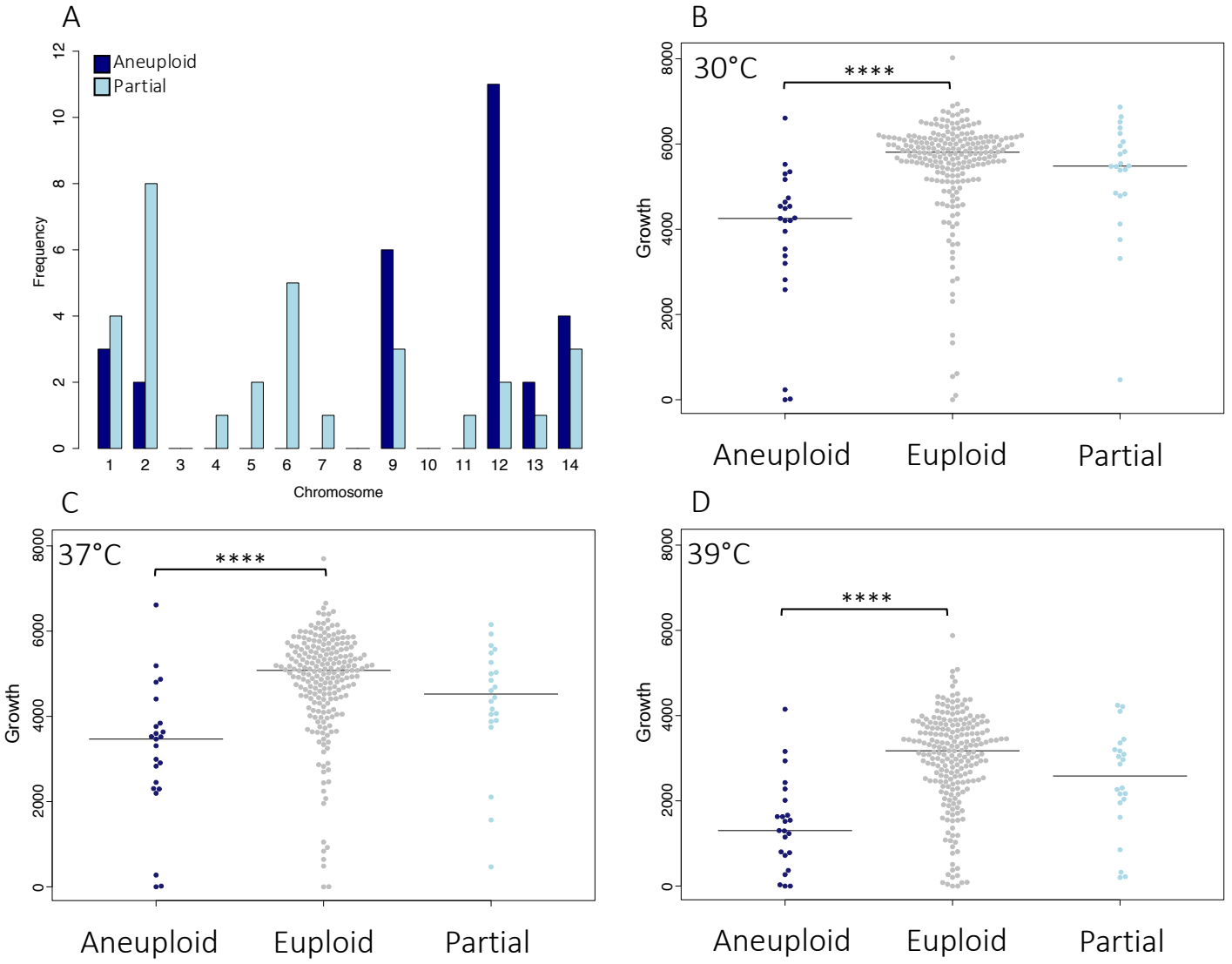


Figure 5. A) Whole (aneuploid) and partial chromosomal duplication frequency throughout the population, by chromosome. Colony size (growth) on YPD, by ploidy state at B) 30°C, C) 37°C. D) 39°C.